Phys Chem Minerals (2006) 33: 207–216
DOI 10.1007/s00269-006-0067-0

ORIGINAL PAPER

Cristiane Castañeda · Sigrid G. Eeckhout
Geraldo Magela da Costa · Nilson F. Botelho
Eddy De Grave

Effect of heat treatment on tourmaline from Brazil

Received: 11 May 2005 / Accepted: 31 January 2006 / Published online: 17 March 2006

Abstract The crystal-chemical behaviour of tourmaline from Araçuaí, Minas Gerais state, Brazil, when subjected to heating in air atmosphere has been studied by several techniques, including EMPA, UV–Vis, TGA, and Mössbauer spectroscopy. The tourmaline samples are typically intermediate members of the elbaite-schorl series. The origin of colour and of its change after treatment has been discussed in terms of local disorder, presence of metal transition elements, oxidation of ferrous iron at the octahedral site, and simultaneous trap of the excess electron. These findings may be used to enhance the colour in tourmaline crystals or generate wanted colour changes.

Keywords Tourmaline · Crystal chemistry · Colour · Heat treatment

Introduction

Tourmaline is a group of structurally and chemically complex borosilicate minerals with the general formula $XY_3Z_6Si_6O_{18}(BO_3)_3V_3W$, where X = Na^{+}, Ca^{2+}, K^{+}, vacancy (□); Y = Mg^{2+}, Fe^{2+}, Mn^{2+}, Al^{3+}, Fe^{3+}, Mn^{3+}, Cr^{3+}, Li^{+}, Ti^{4+}; Z = Al^{3+}, Mg^{2+}, Cr^{3+}, V^{3+}, V = O^{2-}, OH^{-}, and W = O^{2-}, OH^{-}, F^{-} (Hawthorne and Henry 1999). In the structure, corner-sharing tetrahedra (T site) form hexagonal rings and are mainly occupied by Si, although, minor amounts of Al are found in some cases (Rosenberg and Foit 1979). Boron is in triangular coordination and might be substituted by Fe^{3+} (Ja 1972). More recent publications mention the substitution of B for Si at the tetrahedron (Ertl et al. 2001; Hughes et al. 2000; Schreyer et al. 2000, 2002). The Y and Z octahedral sites share edges to form brucite-like fragments. The Z octahedra also share edges with other Z octahedra in a helical linkage parallel to the *c* axis (Burns et al. 1994; Donnay and Barton 1972; Grice and Ercit 1993; Hawthorne 1996). OH groups can occupy two structurally distinct positions, viz., the centre of the hexagonal rings (OH_1), and the corner of brucite-like fragments of three edge-sharing octahedra (OH_3) (e.g., Fig. 1 from Castañeda et al. 2000). These structurally distinct positions have been assigned to two sites, viz., the W-site, which is dominated by OH^{-} [O(1)], F^{-} or O^{2-} and the V-site, which is dominated by OH^{-} [O(3)] or, more rarely, O^{2-} (Hawthorne and Henry 1999).

Tourmaline displays a unique splendour of colours and is frequently used as a gem. Colour and transparency are the most important aspects of the beauty of a gemstone and a significant contributor to a gemstone's value. Hence, gem treatment is a field of high potential wherein less attractive gemstones are transformed to more desirable stones by various methods such as heating, chemical treatment, diffusion, fracture filling, and irradiation.

Some studies on thermal treatments of tourmaline have previously been reported (e.g., Bershov et al. 1969; Sinkankas 1981; De Camargo and Isotani 1988; Nassau 1994), however, no successful enhancement was obtained. This is due to the lack of qualitative results in order to explain the physical processes involved. In view of the complex tourmaline structure, which can incorporate total or partial substitution a great variety of elements, the slightest changes in the composition

C. Castañeda (✉)
Centro de Pesquisa Manuel Teixeira da Costa/IGC/UFMG,
Av. Antônio Carlos, Campus Pampulha, CEP 31270-901,
Belo Horizonte, Brazil
E-mail: ccastaneda@igc.ufmg.br
Fax: +55-31-34994040

S. G. Eeckhout · E. De Grave
Department of Subatomic and Radiation Physics,
Ghent University, Ghent, Belgium

G. M. da Costa
Departamento de Química/ICEB/UFOP, Ouro Preto, Brazil

N. F. Botelho
Instituto de Geociências/UnB, Brasilia, Brazil

Present address: S. G. Eeckhout
European Synchrotron Radiation Facility, Grenoble, France

might result in completely different colours. For Mn-rich tourmaline, the yellow (brown) colour has been attributed to the presence of Mn^{2+} (Ertl et al. 2003) and to Mn^{2+}–Ti^{4+} intervalence charge transfer (Rossman and Mattson 1986), whereas the pink colour has been related to the presence of both Mn^{2+} and Mn^{3+} alone (Donnay 1969; Manning 1973), or in a charge transfer process (Leckebusch 1978; De Camargo and Isotani 1988). Furthermore, Dunn (1975) and Chaudhry and Howie (1976) observed that some pink tourmaline does not contain manganese. Optical absorption spectroscopy revealed that the blue colour in iron-bearing tourmaline is caused by Fe^{2+}–Fe^{3+} (Faye et al. 1974; Leckebusch 1978; Mattson and Rossman 1987; Taran and Rossman 2002) or Fe^{2+}–Ti^{4+} intervalence charge transfer (Rossman and Mattson 1986). In Mössbauer spectra (MS), contributions representing electron delocalization between Fe atoms in adjacent octahedra have been reported for blue, green, and black tourmaline samples (e.g., Hermon et al. 1973; Saegusa et al. 1978; Burns 1982; Mattson and Rossman 1987; da Costa et al. 1997, 1998; Dyar et al. 1998; Eeckhout et al. 2004; Ferrow et al. 1988; Fuchs et al. 1995).

The objective of this study is to document and discuss the heat treatment in pink, blue, and green tourmaline samples from Araçuaí, Brazil. The mineralogical study of the selected crystals was carried out with a variety of techniques, in particular electron-microprobe analyses (EMPA), UV-Vis spectroscopy, thermogravimetric analysis (TGA), and Mössbauer spectroscopy. The combination of these techniques allowed the crystal-chemical characterization of the tourmaline samples, the determination of the temperature at which the samples undergo major modifications, the identification of the origin of colour, and of the change in colour after treatment.

Geological setting, materials and methods

Different populations of granitic pegmatites have been defined in the northeast of the Minas Gerais state, Brazil (Morteani et al. 2000). The pegmatites belong to the Eastern Gemological Province and were formed by partial melting of metasedimentary rocks during the granitogenetic episode of the Neoproterozoic Araçuaí Belt that occurred from 530 to 520 Ma (Pedrosa-Soares and Wiedemann-Leonardos 2000; Pinto and Pedrosa-Soares 2001). Tourmaline samples showing pink (MR2 and MR3), green (CAVG and CAVC), blue (CAAC), and black (MR4) colours, were carefully collected from the complex, zoned Morro Redondo and Jatobá pegmatites, which belong to the Araçuaí Pegmatitic District, NE Minas Gerais state.

The chemical composition of the monocrystalline tourmalines was previously determined by Castañeda et al. (2000). FeO obtained by microprobe was converted to FeO + Fe_2O_3 based on the results of the Mössbauer study. For the elbaite members, the amount of Li^+ was calculated to fill the Y-site as described by Burns et al. (1994). All Mn was assumed to be divalent, in accordance with the UV–Vis, and EPR results (Krambrock et al. 2002).

For the UV–Vis spectroscopic measurements, platelets oriented parallel and perpendicular to the c axis were measured before and after treatment using a Hitachi U3501 spectrophotometer in the spectral region 200–850 nm.

Simultaneous thermal analyses, TGA/DTA, were performed on TA Instruments SDT2960 module using powdered samples. All measurements were done in air and under a N_2 stream of 50 ml/min between room temperature and 1,200°C at a heating rate of 10°C/min.

In our heating treatments two types of experiments were done on natural pink, blue, and green tourmaline samples. The first one was performed on samples in an air furnace for 2 h at 800 and 900°C, 12 h at 110, 450, 700°C, and 48 h at 700°C. The temperature was controlled by a thermocouple and a Eurotherm 818S instrument. For each experiment, the heating rate was 10°C/min, and temperature stabilized within ~5°C. The cooling down, however, was slow and took about 12 h. The second type of experiment the natural pink and blue samples were also subjected to diffusion treatments, in which the samples were involved in a powder consisting of a colouring agent such as Mn, Cu, Cr, and Ti oxides, put in an enclosed space and then placed in a tubular furnace at 700°C for 12 and 48 h.

Mössbauer spectra were collected at room temperature on green and blue tourmaline samples, before and after heat treatment, using standard transmission equipment and a ^{57}Co(Rh) source. A triangular source motion was applied and counts were stored in 1,024 channels. Typically, the number of off-resonance counts per channel (background) was 10^6. The absorbers were prepared by sealing hand-powdered sample in an iron-free sample holder with a styrofoam–benzene mixture. The velocity scale of the spectrometer was periodically calibrated using a spectrum of α-Fe. The velocity increment per channel was ~0016 mm/s. All centre-shift values quoted hereafter are relative to α-Fe.

Results and discussion

Chemical composition

Electron-microprobe analyses are given in Table 1, from which it can be seen that all the samples are intermediate members of the elbaite-schorl series. They contain significant amounts of Fe and Mn, and minor quantities of Mg and Ti. Other elements, such as Co (18 ppm in green sample), and Zn (0.10–0.58 wt% in green and blue samples, respectively) were detected in subordinate concentrations in some samples.

Table 1 Microprobe analyses (wt%) of pink (MR3), blue (CAAC), and green (CAVG and CAVC) tourmaline

	Pink (MR3)	Blue (CAAC)	Green (CAVG)	Pale green (CAVC)
SiO_2	38.02	3738	36.94	37.32
TiO_2	0.01	0.01	0.08	0.01
Al_2O_3	44.16	38.74	38.57	39.53
FeO	0.02	2.64	3.23	1.26
Fe_2O_3	0.00	0.00	0.00	0.00
MgO	0.00	0.01	0.45	0.00
MnO	0.25	2.01	1.32	2.32
ZnO	0.02	0.20	0.06	0.12
CaO	0.41	0.33	0.55	0.49
Na_2O	1.63	2.51	2.45	2.32
K_2O	0.01	0.02	0.03	0.01
Li_2O	1.26	1.45	1.35	1.44
H_2O^+	3.56	3.70	3.69	3.69
F	0.53	ND	ND	0.01
O = F	0.22	0.00	0.00	0.00
Total	89.67	90.03	88.72	88.51

ND not detected

Mössbauer spectroscopy

Iron in each valence and site experiences a distinct electromagnetic distortion that is discernible through ^{57}Fe Mössbauer spectroscopy. Fe sites can be indicative for the degree of ordering in the structure, since a high degree of cationic ordering implies a low number of non-equivalent Fe sites. The spectra of Fe^{2+}- and Fe^{3+}-bearing tourmaline can be composed of several, strongly overlapping, ferrous, mixed-valence and/or ferric doublets (e.g., Dyar et al. 1998; Oliveira et al. 2002; Eeckhout et al. 2004;). As a consequence, they are very difficult to fit, and no clear consensus on the appropriate fitting model to be applied exists. For the present study, the MS were fit using the Lorentzian model. More details are reported elsewhere (Oliveira et al. 2002).

The hyperfine-interaction characteristics as reflected in the MS are displayed in Fig. 1, for blue and green tourmaline, before and after heat treatment at 700°C for 48 h in air. The deviations between the experimental spectra and those adjusted to the data on the basis of discrete doublets were found to be minor. The hyperfine parameters for blue and green tourmaline are listed in Table 2. They are in good agreement with those reported in previous studies. Two and three ferrous contributions were recognized for green and blue tourmaline, respectively. Considering the results of structure refinement and Mössbauer spectroscopic data of various members of the schorl-dravite series, which do not prove the presence of Fe^{2+} at the Z site (Pieczka et al. 1997; Bloodaxe et al. 1999; Piezcka and Kraczka 2004), these doublets are ascribed to Fe^{2+} at two and three distinct Y sites with different nearest-neighbour coordination environments, arbitrarily designated as Y1, Y2, and Y3 (e.g., Dyar et al. 1998; Oliveira et al. 2002; Eeckhout et al. 2004). The smaller ΔE_Q at room temperature points to the higher distortion of the Y3 site as compared to Y1 and Y2. The Fe^{2+} doublet with QS equal 2.46–2.48 mm/s has been attributed to the $[O_4(OH)_2|R^{2+}(R^{2+}, Fe^{3+})]$ neighbourhoods of Fe^{2+} that with QS in the range 2.15–2.30 mm/s to the $[O_4(OH)_2|R^{2+}Al]$ and $[O_4(OH)F|R^{2+}R^{2+}]$ neighbourhoods that with QS in the range 1.80–1.90 mm/s to the

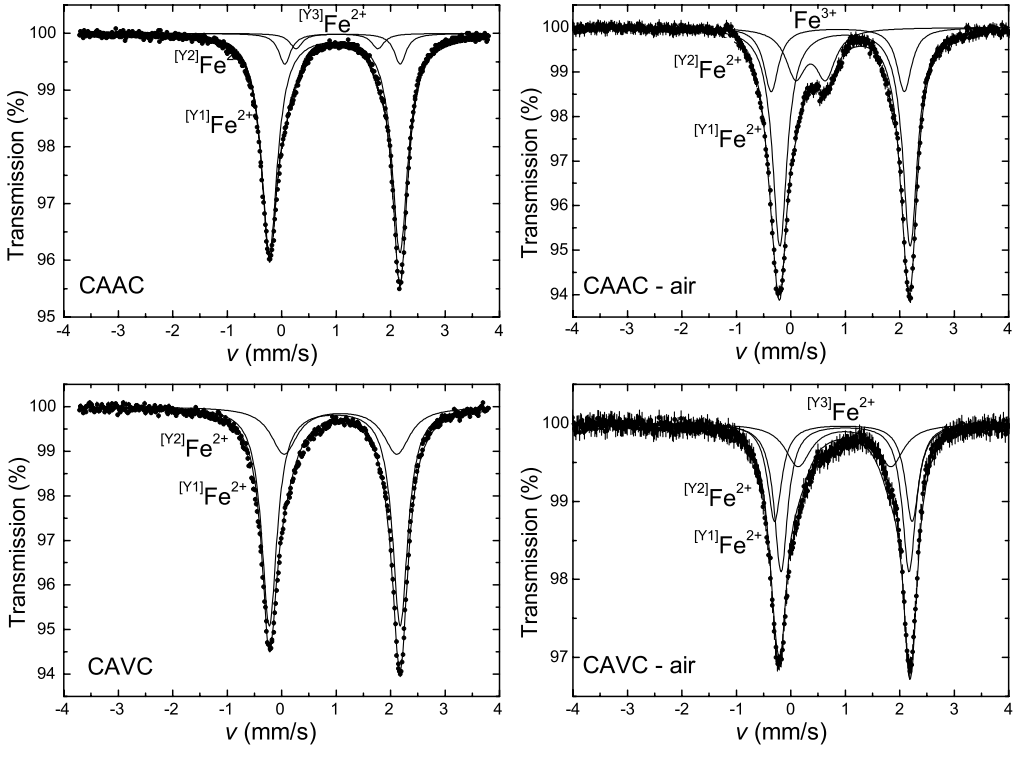

Fig. 1 Experimental (*dots*) and fitted (*solid lines*). Mössbauer spectra at room temperature of blue (CAAC, *top*) and green (CAVC, *bottom*) tourmaline, before (*left*) and after (*right*) treatment at 700°C for 48 h in air

Table 2 Hyperfine parameters at room temperature for blue (CAAC) and green (CAVC) tourmaline before and after heat treatment in air at 700°C for 48 h: quadruple splitting ΔE_Q (mm/s), centre shift δ (mm/s, relative to α-Fe), full width at half maximum Γ (mm/s), and relative area RA (%)

Sample	ΔE_Q	δ	Γ	RA	Assignment
CAAC	2.40 (4)	1.08 (4)	0.36 (1)	86 (2)	Fe^{2+} in Y1
	2.12 (4)	1.22 (4)	0.27 (1)	9 (2)	Fe^{2+} in Y2
	1.50 (4)	1.12 (4)	0.28 (1)	5 (2)	Fe^{2+} in Y3
CAAC (after treatment)	2.44 (4)	0.96 (4)	0.33 (1)	19 (2)	Fe^{2+} in Y1
	2.39 (4)	1.10 (4)	0.33 (1)	63 (2)	Fe^{2+} in Y2
	0.55 (4)	0.47 (4)	0.44 (1)	18 (2)	Fe^{3+} in oct
CAVC	2.43 (4)	1.08 (4)	0.34 (1)	73 (2)	Fe^{2+} in Y1
	2.07 (4)	1.18 (4)	0.59 (1)	27 (2)	Fe^{2+} in Y2
CAVC (after treatment)	2.53 (4)	1.07 (4)	0.31 (1)	31 (2)	Fe^{2+} in Y1
	2.35 (4)	1.10 (4)	0.30 (1)	45 (2)	Fe^{2+} in Y2
	1.71 (4)	1.09 (4)	0.56 (1)	24 (2)	Fe^{2+} in Y3

$[O_4(OH)F|R^{2+}Fe^{3+}]$ and $[O_4(OH)_2|(R^{2+}R^{3+})Ti]$ neighbourhoods and that with QS changing from 1.55 to 1.40 mm/s to the $[O_4(OH)O|R^{2+}(R^{2+},Fe^{3+})]$, and $[O_4(OH)F|R^{2+}Al]$ neighbourhoods (Pieczka and Kraczka 2004). No contributions representing electron delocalization among adjacent Fe^{2+} and Fe^{3+}, nor doublets corresponding to tetrahedrally coordinated ferric iron ions were observed in the MS of the tourmaline samples presently studied (Burns 1982; Dyar et al. 1998).

Heat treatment of the (Fe^{2+}, Mn^{2+}) bearing varieties of tourmaline initiates oxidation above 500–550°C and modifies all the structural polyhedra. The Y octahedra shrink proportionally to the initial content of Fe^{2+} or Fe^{2+} + Mn^{2+}, whereas the thermally induced changes of the mean size of the Z octahedron are less significant. At the final stage of oxidation the transfer of a certain amount of the oxidized Fe^{3+} as well as other ions with larger effective ionic radii than Al from the Y to the Z sites and the equivalent amount of Al in the opposite direction weakens the bonds within the octahedral cluster, leading to the gradual breakdown of the structure between 880 and 920°C (Pieczka and Kraczka 2004). After heat treatment at 700°C (48 h) in air, the overall appearance of the MS for green (CAVC) tourmaline, which consists of a single asymmetric doublet, remains unaltered, whereas an additional contribution is clearly recognized in the blue (CAAC) sample (Fig. 1). The former MS could be satisfactorily fit with three ferrous doublets, viz., Fe^{2+} at Y1, Y2, and Y3, the latter with Fe^{2+} at two distinct Y sites and Fe^{3+} at the octahedral coordination (Table 2). The observed asymmetry within the inner parts of the spectra results from the presence of Fe^{2+} at the Y sites and the temperature- or oxygen fugacity-induced changes in occupancy of the W site by hydroxyl, fluorine, and oxygen, which affect the OH/O ratio as well as the second coordination shell of the Fe^{2+} (Pieczka and Kraczka 2004). Our results imply that heat treatment on green tourmaline produces additional local disorder in the crystal structure, leading to three different ferrous Y sites. Considering the very low iron content of the green sample, no oxidation of the ferrous iron after heat treatment has been observed. For the blue sample, the relative area of Fe^{2+} at Y1 and Y2 changed after heating. At the same time, ferrous iron is no longer present at Y3, and some Fe^{2+} oxidized to Fe^{3+}. It is tempting at this point to ascribe the ferric iron to the highly distorted Y3 site; however, site assignment for Fe^{3+} based on Mössbauer results might be questionable (e.g., Dyar et al. 1998). Furthermore, former Mössbauer results on oxidation in tourmaline show the Fe^{2+} doublets with QS > 2 mm/s to be the first to disappear and the doublets with QS < 2 mm/s to disappear later (e.g., Perfilýev et al. 1973). Such behaviour could indicate faster oxidation of Fe^{2+} at Y sites in which the Fe^{2+}–OH bonds are weaker. However, considering the complex composition of tourmalines, which is the result of numerous coupled substitutes, the observed changes in MS can properly be explained by a progressive evolution of the octahedral clusters involving the coupled exchange of ions at the Y, Z, W, and V sites (Pieczka and Kraczka 2004). In order to determine the Fe^{2+}/Fe^{3+} ratio for heat-treated blue tourmaline, one needs to know the mean difference in Mössbauer fractions, f, for the Fe^{3+} and Fe^{2+} species. Since the calculation of the magnitude of the corrections has not yet been reported for tourmaline, a correction of the areas of ~5% in favour of the Fe^{2+} content has been taken into account. This procedure to calculate the relative populations of the proposed Fe^{2+} and Fe^{3+} sites from the adjusted values of the relative areas of the respective doublets (Table 2) is thought to be reasonable (De Grave and Van Alboom 1991; Eeckhout and De Grave 2003), and results in a Fe^{2+}/Fe^{3+} ratio for heat-treated blue tourmaline of 6.69.

UV–Vis spectroscopy

The absorption bands in the visible spectrum (Fig. 2) were fit using Gaussians, without imposing any additional restrictions. The optical absorption spectrum of green tourmaline ($E \perp c$) shows two small bands at 450 and 470 nm, and a broad, more intense band centred around 720 nm. Blue tourmaline ($E||c$) displays very weak bands at 415, 470, 550, and 600 nm, and a broad, somewhat more intense band centred around 720 nm. The major features of the optical absorption spectrum of

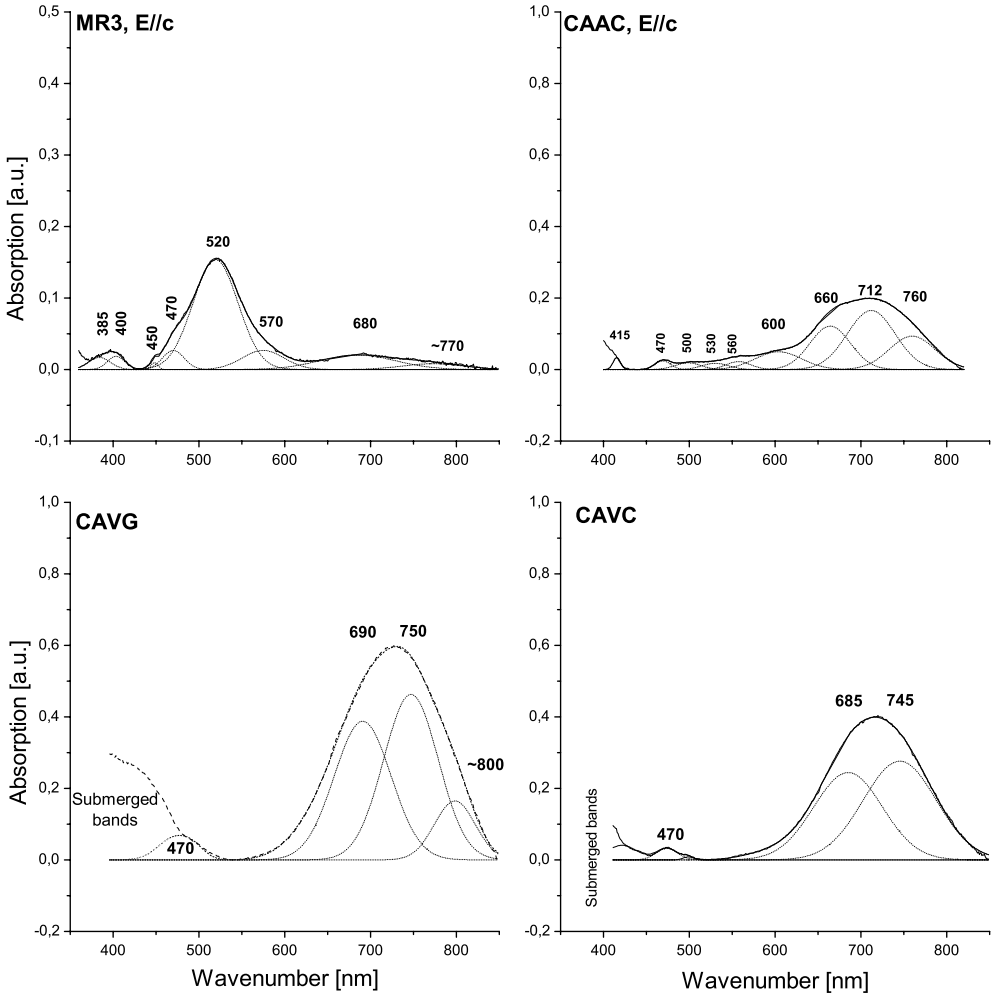

Fig. 2 UV–Vis spectra of pink (MR3), blue (CAAC), and green (CAVG) tourmaline

pink tourmaline ($E||c$) are clearly resolved, rather broad bands around 385, 680, and above 720 nm, together with a dominant, slightly asymmetric band at 520 nm.

Several different interpretations for the band at ~715 nm have previously been suggested. Some authors (Manning 1969; Faye et al. 1974) assigned this band to the $^5T_{2g} \rightarrow {}^5E_g$ transition of Fe^{2+} at the Y site, while others attributed it to the presence of Fe^{2+} at the Z site (Burns 1982; De Camargo and Isotani 1988). Alternative interpretations include Fe^{2+}–Fe^{3+} intervalence charge transfer (Taran et al. 1993; Mattson and Rossman 1987) or even $Mn^{2+} \rightarrow Mn^{3+}$, $Mn^{2+} \rightarrow Fe^{3+}$, $Fe^{2+} \rightarrow Fe^{3+}$ electronic transitions, as well as the presence of Ti^{3+} and Fe^{3+} (Bakhatin et al. 1975). For green and blue tourmaline, the band centred at 720 nm could successfully be fitted using two (at 680 and 745 nm) or three (at ~650, ~700, and ~750 nm) Gaussian lines, respectively. In view of the above-mentioned Mössbauer results, where two or three distinct doublet contributions have been attributed to Fe^{2+} at two or three different Y sites in green and blue tourmaline, respectively, the Gaussian components are caused by Fe^{2+} electronic transitions at two or three different Y sites. Furthermore, the somewhat larger intensity of the band centred at 720 nm in the green sample, as compared to the blue sample, can be related to its slightly larger iron content (Table 1). The additional, weak bands, observed at lower frequency in green (at 470 nm) and blue tourmaline (at 415, 470, 550, and 600 nm) can be attributed to Mn^{2+} (Reinitz and Rossman 1988). The lack of bands at about 520 nm in the green sample can be attributed to the absence of non-magnetic equivalent Mn^{2+} Y sites, impeding the generation of Mn^{2+}–Mn^{2+} colour centres (Krambrock et al. 2002). This might be related to the smaller number of non-equivalent Y sites, as compared to the blue sample. In the latter, the presence of three different, sufficiently distorted Y sites gives rise to the degeneracy, hence, allowing the several iron transitions. These transitions increase the transmission window in the visible area and impede the green transmission, which results in the blue colour. In conclusion, the green colour in Mn–Fe elbaites is related to a smaller degree of disorder as compared to the blue species. Furthermore, this hypothesis might permit to understand the discrepancies that frequently exist between Mössbauer results of blue tourmaline, which only show the presence of ferrous iron, and UV–Vis spectroscopy, where the bands

contributing to the blue colour are attributed to Fe^{2+}–Fe^{3+} charge transfer.

The dominant, slightly asymmetric band at 520 nm in pink tourmaline was successfully decomposed into four Gaussian components, viz., at 450, 470, 520, and 580 nm. These bands, together with the smaller broad bands at 385, 400, and 680 nm can be attributed to the presence of Mn^{2+} ions at the octahedral site (Rossman and Mattson 1986; Reinitz and Rossman 1988). No bands previously assigned to Mn^{3+}, were observed in the presently studied tourmaline samples (Manning 1969, 1973; De Camargo and Isotani 1988).

The UV–Vis spectra after heat treatment at 450 and/or 700°C are depicted in Fig. 3. Pink, green, and blue tourmaline become colourless after heat treatment at 450°C, hence, the corresponding peaks disappear. The increase in relative intensity of the peak at ~500 nm for blue tourmaline after heat treatment at 700°C is in agreement with the red colour change.

Thermal analyses

The TGA curves, as well as their derivatives (DTG), of pink, green, and blue tourmaline are displayed in Fig. 4. The TGA/DTA curves for pink and green tourmaline are similar. They show a minor endothermic loss of weight of 0.50 and 0.16%, respectively, at low temperature and a major endothermic loss of weight of 4.29 and 3.81%, respectively, at high temperature. The TGA curve for the blue sample is characterized by three regions, corresponding to the endothermic losses of weight of 1.87, 2.67, and 3.73% when going from room temperature to 1,200°C. The major, high-temperature loss of weight occurs in one step in the green sample and in two overlapping steps without forming a real plateau in the blue sample. The same features are observed in the DTG curves with maxima at 953°C for green tourmaline, at 964°C for pink, and at 901°C in blue tourmaline. In addition, the high temperature derivative is very narrow for green tourmaline, slightly asymmetric for pink tourmaline, and has a shoulder for the blue sample. Similar behaviours were observed in air and under a N_2 stream of 50 ml/min. The TGA data recorded in air for black tourmaline shows a smaller loss of weight, viz., 0.08% at low temperature and 2.11% at high temperature. The maximum of the DTG curve occurs at 1,000°C.

The drop in mass of 0.50 and 0.16% occurring at low temperature in pink and green tourmaline, respectively, can be ascribed to the expulsion of free, adsorbed water. In blue tourmaline, the drop in mass at similar temperatures is much higher, viz., 1.87%, and followed by another loss of weight of 2.67% situated between 200 and 400°C. These are interpreted as a result of the presence of small fluid inclusions in the mineral, together with some minor amounts of adsorbed water. For all studied tourmaline samples, the major drop in mass of ~4% in the 800–1,000°C temperature interval is most likely due to the release of structurally bound H_2O and OH groups. This proposition is based on the fact that at temperatures close to 1,000°C, tourmaline breaks down completely, generating mullite ($Al_6Si_2O_{13}$). Although this explanation is quite plausible, the inexistence of any other literature data requires further work to fully understand the mechanism of the thermal decomposition of tourmaline.

The observation that this loss of weight occurs in one single step in pink and green tourmaline, and in two overlapping steps in blue tourmaline can be related to the measured FTIR bands in the O–H stretching region performed on these samples (Castañeda et al. 2000). For pink and green tourmaline, three well-defined OH bands were observed, which were assigned to one OH_1 and two OH_3 sites with different surroundings, whereas blue tourmaline was characterized by four sharp, OH bands, consisting of two OH_1 and two OH_3 sites with different environments. This interpretation is corroborated by the behaviour of the black tourmaline sample. The markedly smaller drop in mass of 2.11%, when compared to

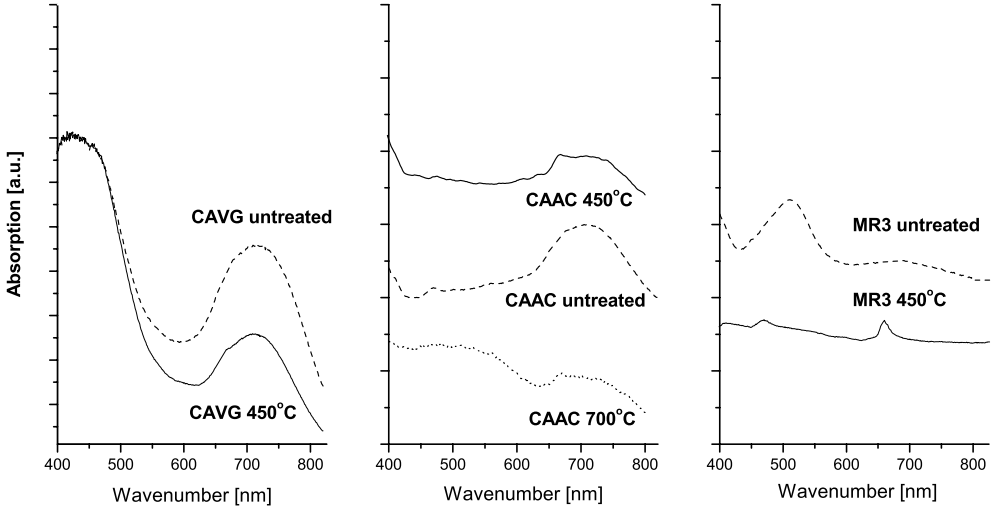

Fig. 3 UV–Vis spectra of pink (MR3), blue (CAAC), and dark green (CAVG) tourmaline after heat treatment in air atmosphere

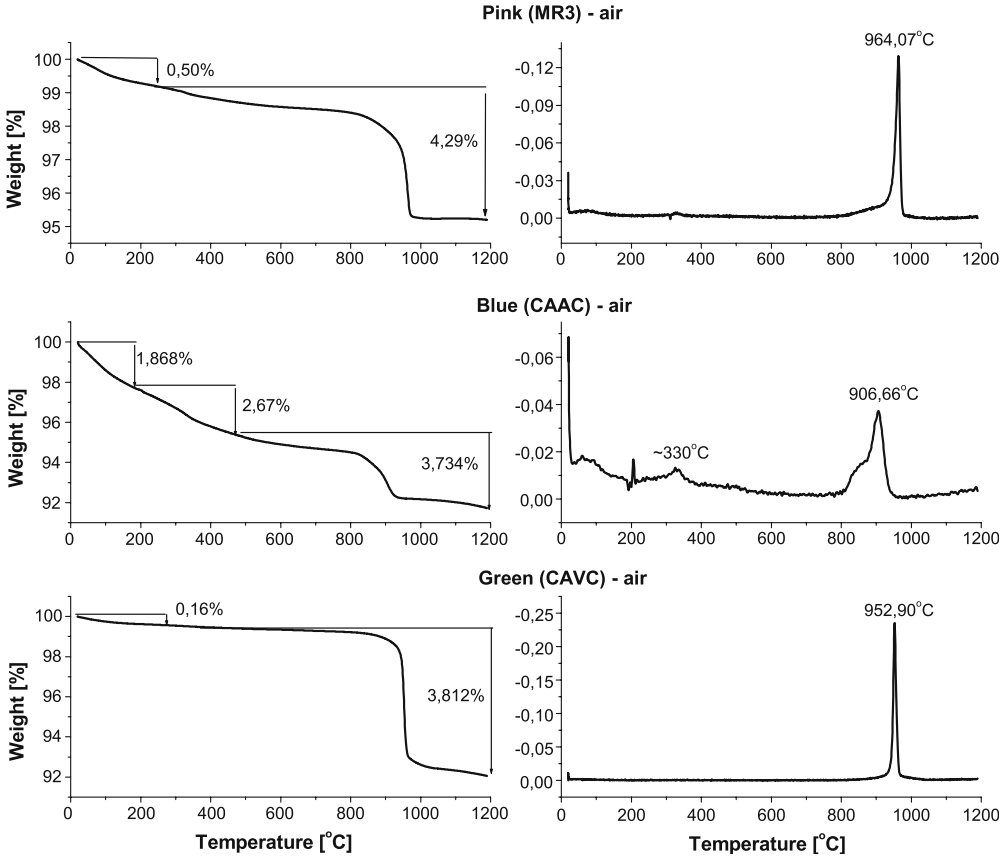

Fig. 4 TGA/DTG curves of pink (MR3), blue (CAAC), and green (CAVC) tourmaline

the other studied tourmaline samples, can be related to the observed, broad O–H stretching bands. The latter feature can be attributed to order–disorder phenomena, which are governed by charge balance and bulk chemistry and, hence, by the geological environment (Oliveira et al. 2002). This interpretation is further corroborated by Fuchs et al. (2002), who reported that the oxidation of Fe^{2+} is linked to the deprotonation of the OH_1 group. The drop in mass can thus be related to concomitant deprotonation and oxidation phenomena, both favoured by order–disorder phenomena. In addition, all tourmaline samples show two FTIR bands, assigned to structural H_2O (Castañeda et al. 2000).

Heat treatment

The results of the heat treatments on pink, blue, and green tourmaline are mentioned in Table 3. In air experiments, pink and blue tourmaline become colourless when heated at 110 or 450°C for 12 h. The original pink colour, with minor variations of its intensity at surface fractures, is recovered after heat treatment at 700°C for both 12 and 48 h, whereas the blue sample becomes greyish, violet and red, respectively. With the increasing temperature, the green sample labelled CAVG changes after 12 h to pale green (at 110°C), to brown (at 450°C), and dark brown (at 700°C), whereas sample CAVC passes from yellowish green to colourless, and grey, respectively. With increasing duration (48 h) at 700°C, CAVG remains dark brown, whereas CAVC becomes bluish grey. In order to verify whether the different behaviours upon heat treatment imply that subtle crystal chemical variations might affect the observed colour changes, a pink tourmaline from Governador Valadares with unknown crystal chemistry, was subjected to heat treatment at 700°C for 48 h. This pink sample turned to green, hence confirming the effect of crystal chemistry and, thus, of geological environment. Pink, blue, and green tourmaline subjected to thermal treatments at 800 or 900°C for 2 h become milky and show a large amount of surface fractures. These observations are completely in line with the TGA/DTG data, where a major drop in mass of ~4% in the 800–1,000°C temperature interval has been observed, which can be ascribed to the release of structurally bound H_2O and OH groups.

Furthermore, the duration of heat treatment is a controlling parameter in the heat treatment of tourmaline, where durations exceeding 48 h favour the fracturing of the crystals, producing milky features and colour change in the blue sample.

Diffusion treatment

In an attempt to produce a specific colour enhancement by diffusion heat treatment (Table 4), pink tourmaline

Table 3 Results of the heat treatments in air atmosphere on pink (MR3), blue (CAAC), and green (CAVG and CAVC) tourmaline, with *T* the temperature in °C and time the duration in hours

Sample	*T*	Time	Results	Products
MR3	110	12	Lightness	Colourless
CAAC			Lightness	Almost colourless
CAVG			Lightness	Pale green
CAVC			Lightness + colour change	Yellowish green
MR3	450	12	Clear up	Colourless
CAAC			Clear up	Colourless
CAVG			Lightness + colour change	Pale brown
CAVC			Clear up	Colourless
MR3	700	12	Lightness + colour change	Pale pink with dark pink shadow
CAAC			Colour change	Greyish violet
CAVG			Colour change	Dark brow
CAVC			Colour change	Greyish
MR3	700	48	Lightness + colour change	Pale pink with dark pink shadow
CAAC			Colour change	Dark red
CAVG			Colour change	Dark brown
CAVC			Darkness	Bluish grey
MR3	800 or 900	2	Milky samples with high amounts of fractures and new products	
CAAC				
CAVG				
CAVC				

was put in contact with Cr, Mn, and Cu oxides, the latter to try to create the attractive colour of Paraíba tourmaline. Blue and green species were put in contact with Cr oxide to increase the green hues, and with Ti oxide to reverse the yellow colour.

The diffusion treatments at 700°C on blue tourmaline resulted in a variety of colour changes in the presence of Cr or Ti oxide, depending on the duration of the treatment. After 12 h, a greyish-violet colour was observed, which changed to red after 24 h and became dark red after more than 72 h. On the other hand, similar treatments on pink tourmaline in Cr, Mn, or Cu oxide produced no remarkable colour changes, and only slight variations on the intensity of the pink colour were revealed at surface fractures. These colour changes for both blue and pink tourmaline are comparable to the ones observed after heat treatment in air and are observed through the whole crystal. As a consequence, they cannot be attributed to diffusion. In addition, these preliminary results point to the lack of any relation between colouring agent and observed colour change.

Concluding remarks

The origin of colour in pink tourmaline can be attributed to the presence of Mn^{2+} at different, magnetically non-equivalent, distorted octahedral sites. No enhancement colour changes were observed after heat treatment, implying that this ion remains divalent. Concomitantly, the ferrous iron ions did not oxidize upon heating. The green colour in tourmaline is related to the presence of

Table 4 The results of the heat treatments in air in an enclosed space filled by Mn, Cu, Cr, and Ti oxides on pink (MR3), blue (CAAC), and green (CAVG) tourmaline. Temperature (*T*) is expressed in °C and time in hours

Sample	Oxide	*T*	Time	Results	Products
MR3	Cr	700°C	12	Lightness + colour change	Pale pink with dark pink shadow
			24	Colour change	Dark pink located in grooves
			72	Colour zonation	Dark pink located in grooves
CAAC	Cr	700°C	12	Colour change	Greyish violet
			24	Colour change	Red
			48	Colour change	Red
			>72	Colour change + darkness	Dark red
MR3	Mn or Cu	700°C	12	The same change as in air experiments	
			48		
CAAC	Ti	700°C	12	Colour change	Greyish violet
			48	Colour change	Red
CAVG	Cr or Ti	700°C	12	The same change as in air experiments	
			48		

ferrous iron at the octahedral site. Heating produces additional local disorder in the crystal structure, resulting in three different ferrous Y sites and causing the change in colour from green to brown or bluish grey. Furthermore, the green colour in Mn–Fe elbaites is related to a smaller degree of disorder as compared to the blue species.

The transformation of blue tourmaline into red tourmaline after heat treatment in air at 700°C for 48 h involves two phenomena: (1) structural adjustments of the tourmaline crystal accompanied by the part oxidation of ferrous iron at the octahedral site, and (2) simultaneous trap of the excess electron. This electron can be captured by the H^+ ion of the molecular H_2O present, involving the breakdown of the water molecule, and the liberation of OH^-. This is completely in line with the TGA/DTG data, where the major loss in weight of ~4% occurs less abruptly in the blue tourmaline than in green tourmaline (Fig. 2).

In conclusion, the physico-chemical mechanisms of colour transformations in tourmaline from Araçuaí, Brazil, induced by heating, have been unambiguously demonstrated by combining several techniques. Moreover, these findings may be used to enhance the colour in tourmaline or generate wanted colour changes. Dark green and dark blue tourmaline can benefit from heating at low temperatures in air by producing lighter colourations. Furthermore, after a long heat treatment at 700°C in air, blue tourmaline transforms to red. Pink tourmaline does not profit from any heating procedure.

Acknowledgements The authors are indebted to the Brazilian research-funding agencies Conselho Nacional de Pesquisa (CNPq), CAPES and Fundação Educativa de Ouro Preto (FEOP). Financial support for the Mössbauer study was obtained from the Fund for Scientific Research—Flanders, Belgium, grant G018503. Special acknowledgments go to Dr. A.C.S. Sabione, César Mendonça, and José Davi Cabral from Universidade Federal de Ouro Preto, Brazil. The work benefited from the reviews of Y. Fuchs and an anonymous reviewer.

References

Bakhatin AI, Minko O, Vinokurov VM (1975) Isomorphism and colour of tourmaline. Izv Akad Nauk SSSR Ser Geol 6:73

Bershov LV, Martirossyan VO, Marfunin AS, Plantanov AN, Tarasschan AN (1969) Colour centres in lithium tourmaline (elbaite). Sov Phys Crystallogr 13:629–630

Bloodaxe ES, Hughes JM, Dyar MD, Grew ES, Guidotti CV (1999) Linking structure and chemistry in the Schorl–Dravite series. Am Mineral 84:922–928

Burns RG (1982) The blackness of Schorl: Fe(2+) Fe(3+) electron delocalization in tourmaline. Trans Am Geophys Union 64:1142

Burns PC, MacDonald DJ, Hawthorne F (1994): The crystal chemistry of manganese-bearing elbaite. Can Mineral 32:31–41

Castañeda C, Oliveira EF, Gomes N, Pedrosa-Soares AC (2000) Infrared study of OH sites in tourmaline from the elbaite-schorl series. Am Mineral 85:1503–1507

Chaudhry MN, Howie RA (1976) Lithium tourmalines from The Meldon Aplite Devonshire, England. Mineral Mag 40:747–751

da Costa GM, Castañeda C, Gomes NS, Soares ACP, Santana GP (1997) On the analysis of the Mössbauer spectra of tourmalines. Hyp Interact C 2:29–34

da Costa GM, Castañeda C, Eeckhout SG, De Grave E, Gomes NS (1998) The temperature dependence of the hyperfine parameters of tourmalines. Hyp Interact C 3:344–347

De Camargo MB, Isotani S (1988) Optical absorption spectroscopy of natural and irradiated pink tourmaline. Am Mineral 73:172–180

De Grave E, Van Alboom A (1991) Evaluation of ferrous and ferric Mössbauer fractions. Phys Chem Minerals 18:337–342

Donnay G (1969) Crystaline homogeneity: evidence from electron-probe study of Brazilian tourmalines. Carnegie Inst Washington Ann Dir Geophys Lab 8:219–220

Donnay G, Barton R (1972) Refinement of the crystal structure of elbaite and the mechanism of tourmaline solid solution. Tscher Min Petr Mitt 18:273–286

Dunn PJ (1975) On gem elbaite from Newry, Maine, USA. J Gemmol 14:357–368

Dyar MD, Taylor ME, Lutz TM, Francis CA, Guidotti CV, Wise M (1998) Inclusive chemical characterization of tourmaline: Mössbauer study of Fe valence and site occupancy. Am Mineral 83:848–864

Eeckhout SG, De Grave E (2003) Evaluation of ferrous and ferric Mössbauer fractions Part II. Phys Chem Minerals 30:142–146

Eeckhout SG, Corteel C, Van Coster E, De Grave E, De Paepe P (2004) Crystal-chemical characterization of tourmalines from the English Lake District: electron-microprobe analyses and Mössbauer spectroscopy. Am Mineral 89:1743–1751

Ertl A, Hughes JM, Marler B (2001) Empirical formulae for the calculation of <T–O> and X–O2 bond lengths in tourmaline and relations to tetrahedrally-coordinated boron. N Jb Miner Mh 12:548–557

Ertl A, Hughes JM, Prowatke S, Rossman GR, London D, Fritz EA (2003) Mn-rich tourmaline from Austria: structure, chemistry, optical spectra, and relations to synthetic solid solutions. Am Mineral 88:1369–1376

Faye GH, Manning PG, Gosselin JR (1974) The optical absorption spectra of tourmaline importance of charge-transfer processes. Can Mineral 12:370–380

Ferrow EA, Annersten H, Gunawardane RP (1988) Mossbauer-effect study on the mixed-valence state of iron in tourmaline. Mineral Mag 52:221–228

Fuchs Y, Lagache M, Linares J, Maury R, Varret F (1995) Mössbauer and optical spectrometry of selected schorl-dravite tourmalines. Hyp Interact 96:245–258

Fuchs Y, Lagache M, Linares J (2002) Annealing in oxidising conditions of Fe-tourmalines and correlated deprotonation of OH groups. CR Geosci 334(4):245–249

Grice JD, Ercit TS (1993) Ordering of Fe and Mg in the tourmaline crystal structure. The correct formula. N Jb Miner Abh 165:245–266

Hawthorne FC (1996) Structural mechanisms for light-element variations in tourmaline. Can Mineral 34:123–132

Hawthorne FC, Henry DJ (1999) Classification of the minerals of the tourmaline group. Eur J Mineral 11:201–215

Hermon E, Simkin DJ, Donnay G, Muir WB (1973) The distribution of $Fe^{(2+)}$ and $Fe^{(3+)}$ in iron-bearing tourmalines: a Mössbauer study. Tscher Min Petr Mitt 17:124–132

Hughes JM, Ertl A, Dyar MD, Grew ES, Shearer CK, Yates MG, Guidotti CV (2000) Tetrahedrally coordinated boron in a tourmaline: boron-rich olenite from Stoffhutte, Koralpe, Austria. Can Mineral 38:861–868

Ja YH (1972) $g = 43$ isotropic epr line in tourmaline. Chem Phys (USA) 57(7):320–322

Krambrock K, Pinheiro MVB, Medeiros SM, Guedes KJ, Schweizer S, Spaeth JM (2002) Investigation of radiation-induced yellow color in tourmaline by magnetic resonance. Nucl Instrum Meth B 191:241–245

Leckebusch R (1978) Chemical composition and colour of tourmalines from Darre Pech (Nuristan, Afghanistan). N Jb Miner Abh 133:53–70

Manning PG (1969) Optical absorption spectra of chromium bearing tourmalines, black tourmaline and buerguerite. Can Mineral 10:57–70

Manning PG (1973) Effect of second-nearest-neighbor interaction on Mn^{3+} absorption in pink and black tourmalines. Can Mineral 11:971–977

Mattson SM, Rossman GR (1987) Fe^{2+}–Fe^{3+} interactions in tourmaline. Phys Chem Minerals 14:163–171

Morteani G, Preinfalk C, Horn AH (2000) Classification and mineralization potential of the pegmatites of the Eastern Brazilian Pegmatite Province. Mineral Deposita 35:638–655

Nassau K (1994) Gemstone enhancement history, science and state of the art. 1st edn. St. Edmundsbury Press, Great Britain, p 252

Oliveira EF, Castañeda C, Eeckhout SG, Gilmar MM, Kwitko RR, Botelho NF (2002) Infrared study of Brazilian tourmalines from different geological environments. Am Mineral 87:1154–1163

Pedrosa-Soares AC, Wiedemann-Leonardos CM (2000) Evolution of the Araçuaí belt and its connection to the Ribeira belt, eastern Brazil. In: UG Cordani EJ, Milani A, Thomaz DA Campo (eds) Tectonic evolution of South America, 31st international geological congress, Rio de Janeiro, pp 265–285

Perfilýev YuD, Gorelikhova NV, Babeshkin AM (1973) Oxidation of tourmaline in the 200–1100°C range. Int Geol Rev 20:982–990

Pieczka A, Kraczka J (2004) Oxidized tourmalines—a combined chemical, XRD and Mössbauer study. Eur J Mineral 16:309–321

Pieczka A, Kraczka J, Zabinski W (1997) Mössbauer spectra of Fe^{3+}-poor schorls: reinterpretation of the spectra on a basis of an ordered structure model. In: International symposium on tourmaline, abstract, Nové Mesto na Morave, Czech Republic, pp 74–75

Pinto CP, Pedrosa-Soares AC (2001) Brazilian gem provinces. Austral Gemmol 21:12–16

Reinitz IM, Rossman GR (1988) Role of natural radiation in tourmaline colouration. Am Mineral 73:822–825

Rosenberg PE, Foit FF (1979) Synthesis and characterization of alkali-free tourmaline. Am Mineral 64:180–186

Rossman GR, Mattson SM (1986) Yellow Mn-rich elbaite with Mn–Ti intervalence charge transfer. Am Mineral 71:599–602

Saegusa N, Price DC, Smith G (1978) Analysis of the Mössbauer spectra of several iron-rich tourmalines. In ''ICAME, international conference on the application of the Mössbauer effect, Annais, Kyoto, Japan 1:38–42

Schreyer W, Wodara U, Marler B, van Aken PA, Seifert F, Robert JL (2000) Synthetic tourmaline (olenite) with excess baron replacing silicon in the tetrahedral site: I Synthesis conditions, chemical and spectroscopic evidence. Eur J Mineral 12:529–541

Schreyer W, Hughes JM, Bernhardt HJ, Kalt A, Prowatke S, Ertl A (2002) Reexamination of olenite from the type locality: detection of boron in tetrahedral coordination. Eur J Mineral 14:935–942

Sinkankas J (1981) Gemstone, mineral data book. 2nd edn. Van Nostrand Reinhold Company, New York, p 352

Taran MN, Rossman GR (2002) High-temperature, high-pressure optical spectroscopic study of ferric-iron-bearing tourmaline. Am Mineral 87:1148–1153

Taran MN, Lebedev AS, Platanov NA (1993) Optical absorption spectroscopy of synthetic tourmalines. Phys Chem Minerals 20:209–220